Supporting Material

A pH Dependent Kinetic Model of Dihydrolipoamide Dehydrogenase from Multiple Organisms

Michael A. Moxley,[†], Daniel A. Beard[‡*] and Jason N. Bazil,[‡]

[†]Department of Biochemistry, Biotechnology and Bioengineering Center, Medical College of Wisconsin, Milwaukee Wisconsin; [‡]Department of Molecular and Integrative Physiology, University of Michigan, Ann Arbor, Michigan
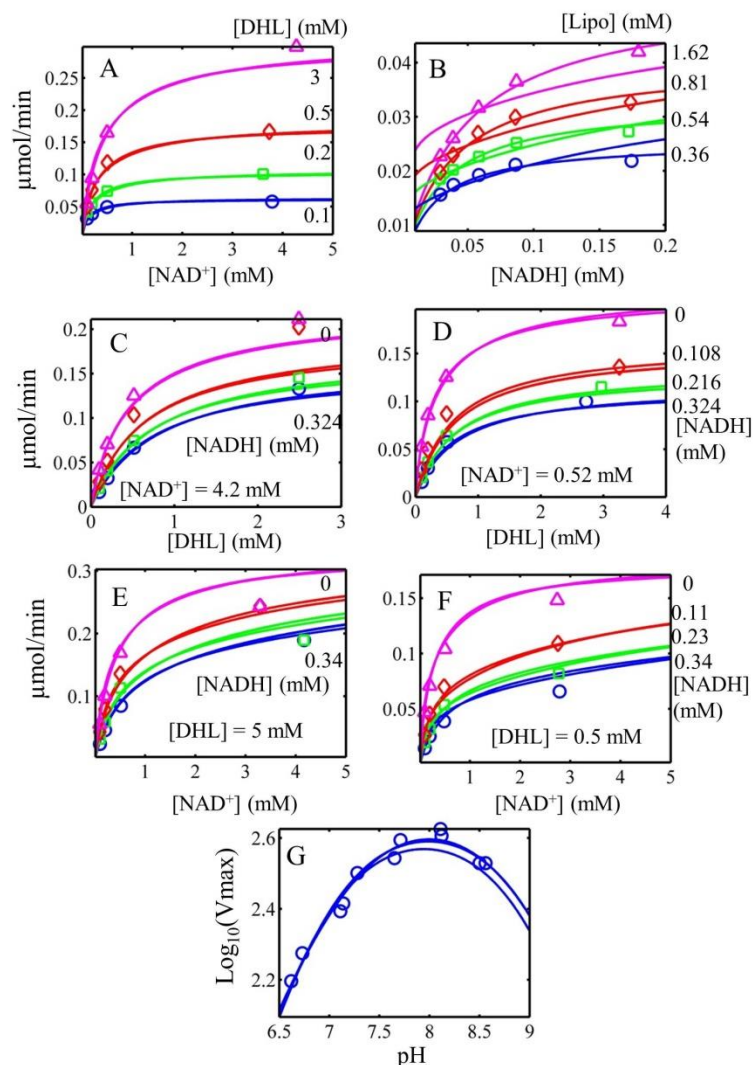
[*]Correspondence: beardda@umich.edu

Figure S1. Multiple global fits of rat liver E3 activity as a function of substrates, products, and pH where data was obtained from (1). Data were fitted to the simple redox independent K_d model through hundreds of trials of global followed by local optimization using random initial parameter values (See methods section) where 127 fits that were within fval(max)/fval(min) of 1.12 were kept. All 127 parameter sets were simulated and shown overlaid with the data. A) Initial velocity data in the absence of products in the forward direction by varying NAD^+ in different fixed concentrations of dihydrolipoamide (DHL) at pH = 8 were obtained from Fig. 1A of (1). B) Initial velocity data in the absence of products in the reverse direction with varied NADH and different fixed lipoamide (Lipo) at pH = 8 were obtained from Fig. 1B of (1). C) Initial velocity data in the forward direction varying DHL in high NAD^+ concentration with different fixed NADH (Top to bottom: 0, 0.108, 0.216, and 0.324 mM) at pH = 8 were obtained from Fig. 3 of (1). D) Initial velocity data in the forward direction varying DHL in low NAD^+ concentration with different fixed NADH at pH = 8 were obtained from Fig. 4 of (1). E) Initial

velocity data in the forward direction at high DHL concentration with different fixed NADH (Top to bottom: 0, 0.11, 0.23, and 0.34 mM) at pH = 8 were obtained from Fig. 5 of (1). F) Initial velocity data in the forward direction at low DHL in different fixed concentrations of NADH at pH = 8 were obtained from Fig. 6 of (1). G) Log10(Vmax) of the forward reaction with pH obtained from Fig. 9 of (1). In all panels, the data are represented by circles, squares, diamonds, or triangles and the model is represented by solid lines of the corresponding color.

Table S1.

²Parameter	Family 1 (Avg of 34 fits)	Family 2 (Avg of 50 fits)	Family 3 (Avg of 43 fits)
Rat liver E3 observed kinetic parameters from multiple fits to data obtained from (1).			
[b]k1 (min^{-1})	4.05×10^4	6.47×10^4	6.27×10^4
k2 (min^{-1})	294	2.92×10^3	2.59×10^3
k3 (min^{-1})	2.56×10^4	2.41×10^4	2.20×10^4
k4 (min^{-1})	10^7	2.26×10^6	2.26×10^6
[b]k5 (min^{-1})	1.22×10^4	1.4×10^4	1.35×10^4
k6 (min^{-1})	5.56×10^3	2.11×10^3	1.85×10^5
k7 (min^{-1})	1.33×10^5	5.98×10^4	5.48×10^4
k8 (min^{-1})	8.30×10^5	1.67×10^4	1.68×10^4
pKh1 (thiolate)	6.98	6.89	6.89
pKh2 (base)	9	8.8	9
Ka (mM)	0.920	1.51	1.47
Kb (mM)	1.74	0.907	0.935
Kp (mM)	0.757	0.707	0.7051
Kq (mM)	1.24	0.228	0.231
[c]Keq	0.206	0.0278	0.0283
[d]Fval (cost function)	0.359	0.401	0.402

[a]Rate constants were given a boundary of 10^{-3} to 10^9 min^{-1} and equilibrium dissociation constants were bounded by 1 to 10^4 μM. pKh1 and 2 were generally bounded by values between 4 and 9.

[b]These rate constants were calculated based on equilibrium detailed balance constraints derived in the methods section.

[c]The fitted equilibrium constant for this data set was allowed to vary more than others because this data was collected at 37 °C whereas other data shown was collected at 25 °C with a known equilibrium constant reported previously (2).

[d]The cost function value was calculated through the weighted global sum of squares described previously (3).
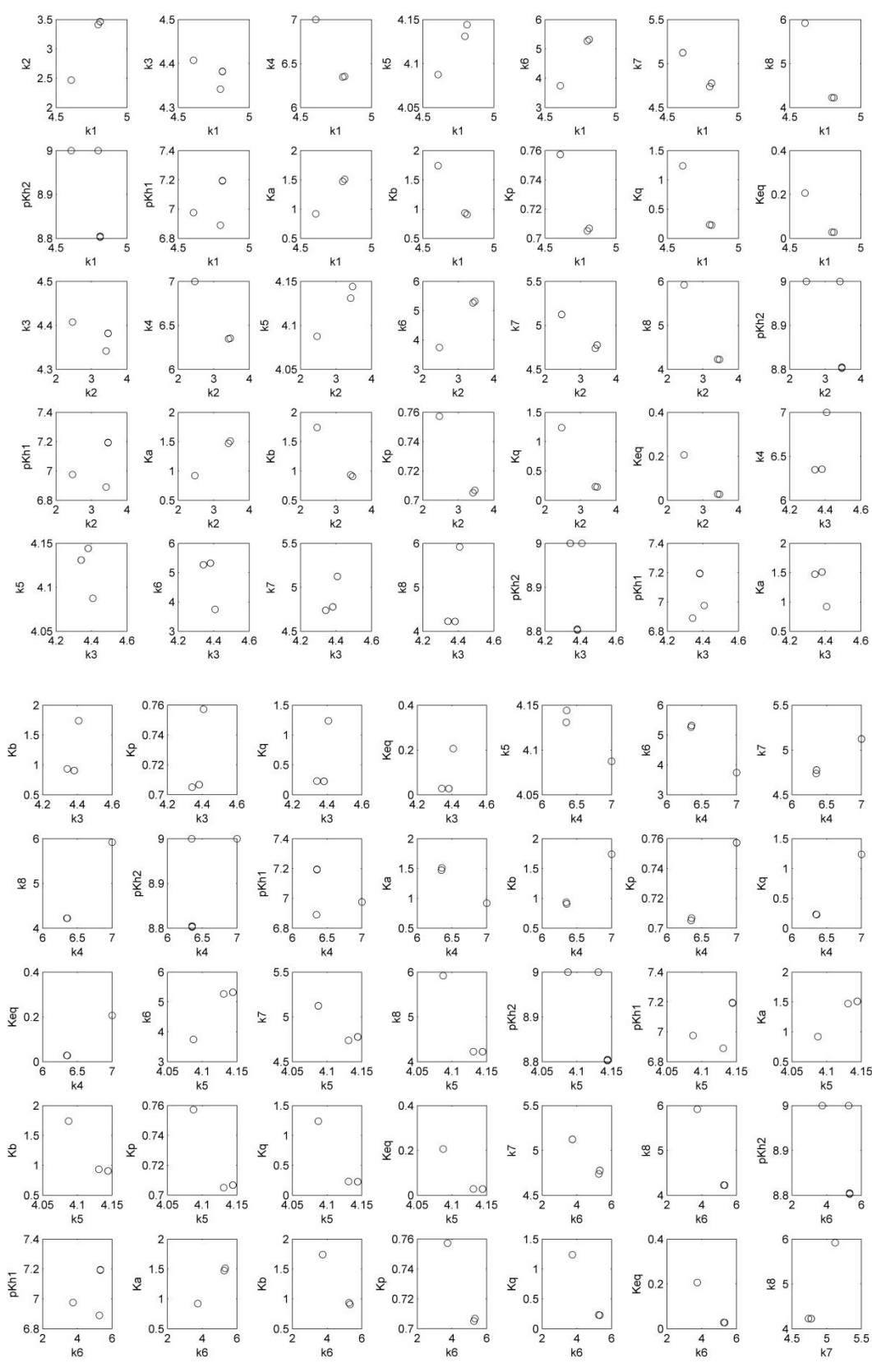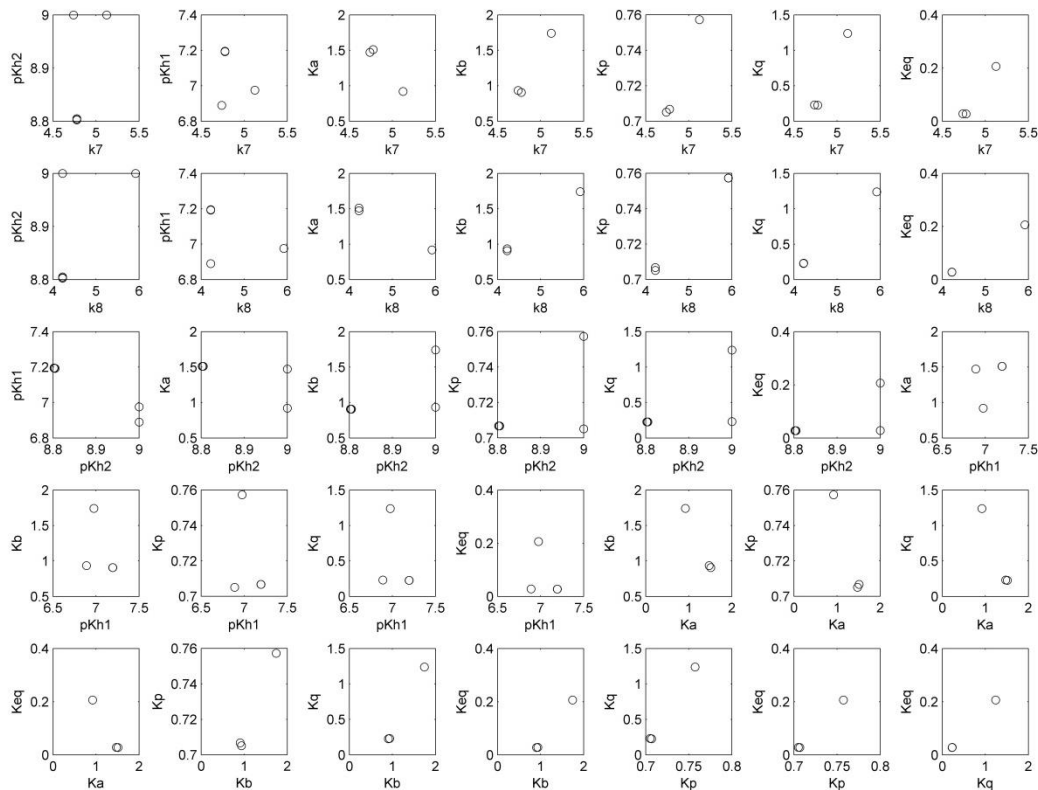
Figure S2. Scatter plots of Rat liver E3 kinetic parameters. The kinetic parameters from 127 fits within the max/min cost value range of 1.12 shown in Figure S1 were plotted as all paired parameter combinations. K_A, K_B, K_P, and K_Q are defined as equilibrium dissociation constants for dihydrolipoamide, NAD^+, lipoamide, and NADH, respectively. The overall equilibrium constant (K_{eq}) for the reaction is defined in the main text under Model constraints. All rate constant values (k_1 through k_8) are plotted as $\log_{10}$(rate constant). Rate constants and equilibrium dissociation constants are in units of min^{-1} and mM, respectively.
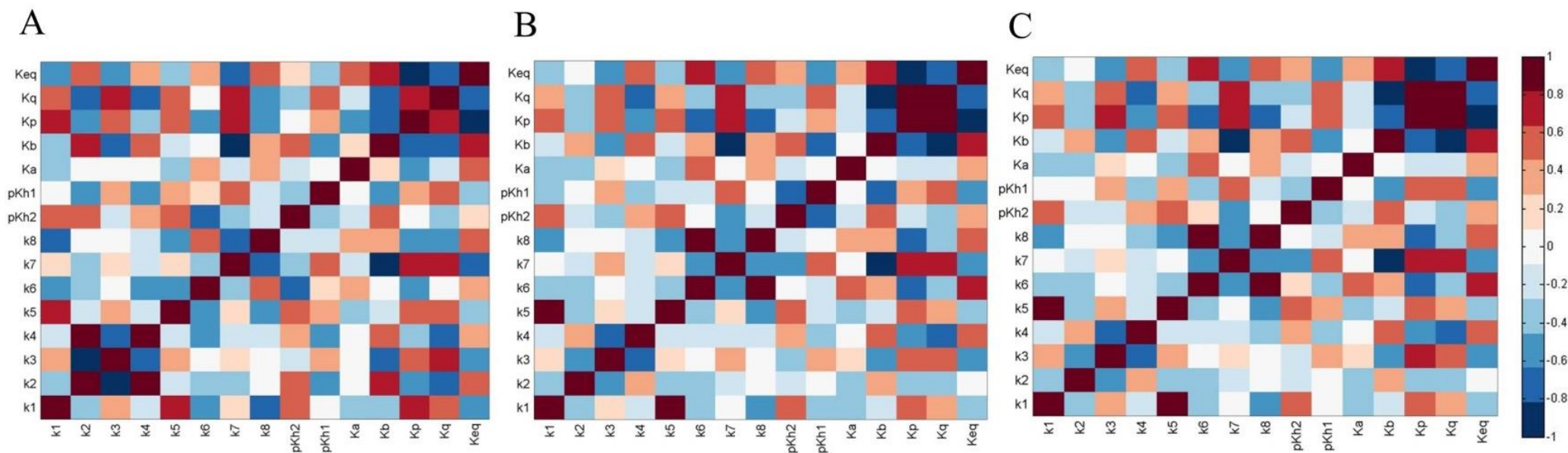
Figure S3. Correlation matrix heat maps of rat liver E3 kinetic parameters. A) Parameter correlation matrix for parameter family 1 shown in Table S1. B) Parameter correlation matrix for parameter family 2 shown in Table S1. C) Parameter correlation matrix for parameter family 3 shown in Table S1. K_A, K_B, K_P, and K_Q are defined as equilibrium dissociation constants for dihydrolipoamide, NAD^+, lipoamide, and NADH, respectively; K_{eq} is the overall equilibrium constant for the reaction defined in the main text under Model constraints. pKh1 and pKh2 correspond to the thiolate and the base, respectively.
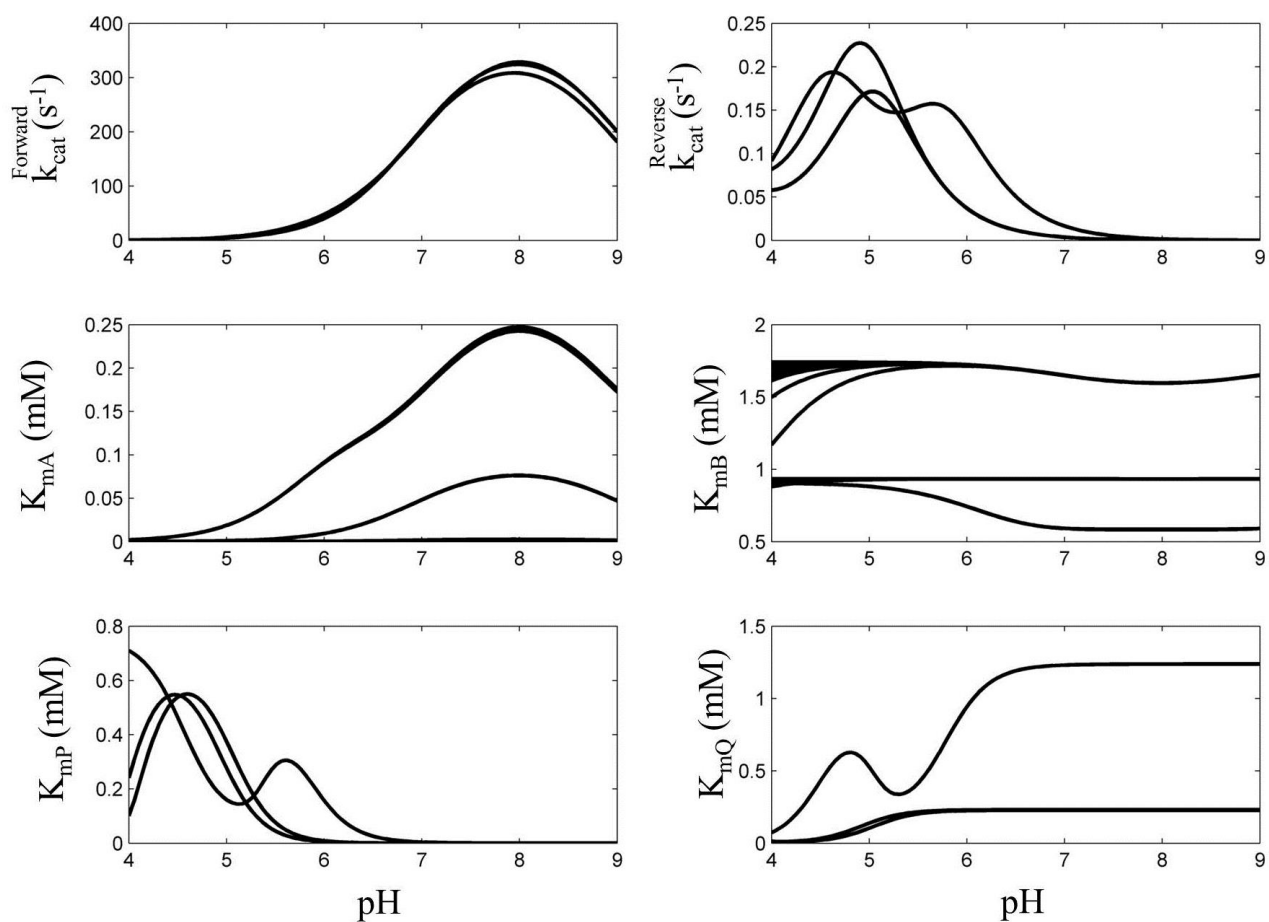
Figure S4. Rat liver E3 calculated steady-state parameters (using all 127 parameters sets that were within fval(max)/fval(min) of 1.12) as a function of pH using the redox independent single Kd model. K_{mA}, K_{mB}, $K_{mP,}$ and K_{mQ} are the Michaelis constants for dihydrolipoamide, NAD^+, lipoamide, and NADH, respectively.
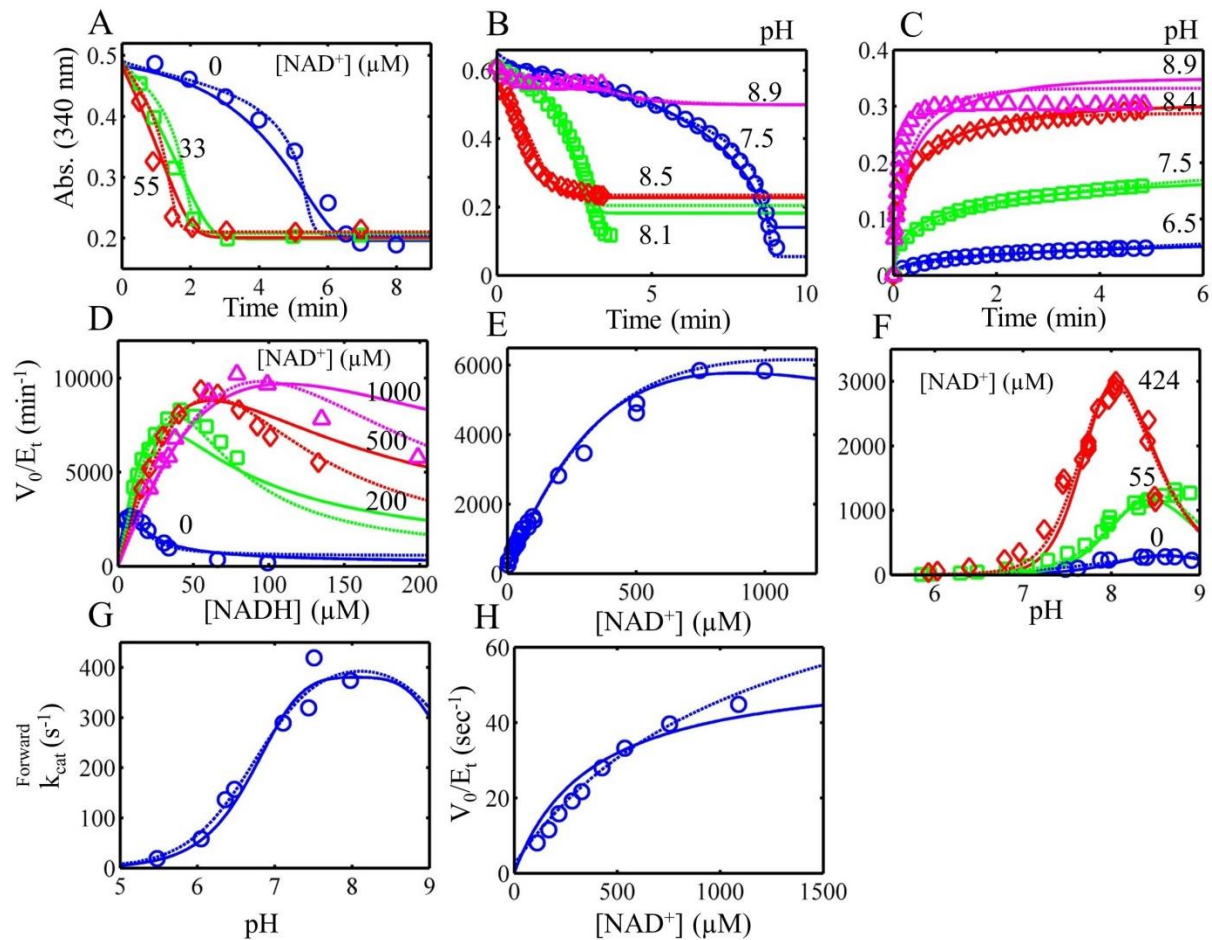
Figure S5. Redox independent K_d (solid lines) and redox dependent K_d (dashed lines) models fitted to *E. coli* E3 data with Keq values of 0.05 and 0.048, respectively.
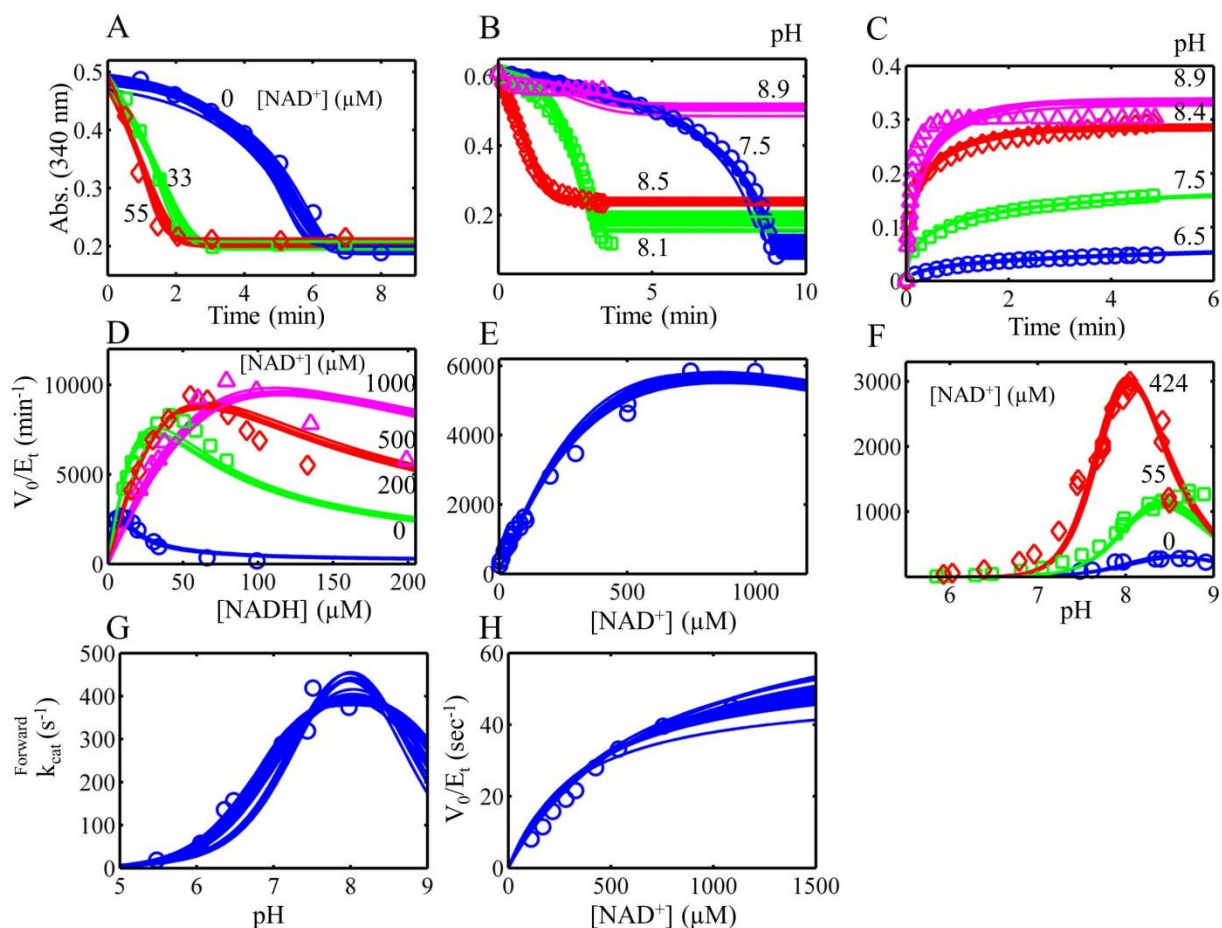
Figure S6. Multiple global fits of *E.coli* E3 progress curve, substrate inhibition, NAD^{+} activation, and pH-dependent data obtained from (4-6). Data were fitted to the simple redox independent K_d model through hundreds of trials of global followed by local optimization using random initial parameter values (See methods section) where 100 fits that were within fval(max)/fval(min) of 1.26 were kept. A) Progress curves for the reverse reaction (pH = 7.9) in different NAD^{+} concentrations where the data was obtained from Fig. 1 in (4). B) Progress curves for the reverse reaction in varying pH where the data was obtained from Fig. 5 of (5). C) Progress curves in the forward direction with varying pH where the data was obtained from Fig. 4 of (5). D) Initial velocity divided by total enzyme concentration (v_0/E_t) in the reverse direction (pH = 7.9) with varied NADH with different fixed NAD^{+} concentrations where the data was obtained from Fig. 6 in (4). E) Activation of reverse v_0/E_t (pH = 7.9) with increasing NAD^{+} concentration where the data was obtained from Fig. 3 in (4). F) v_0/E_t as a function pH and NAD^{+} concentration where the data was obtained from Fig. 2 in (4). G) Forward k_{cat} as a function of pH where the data was obtained from Fig. 4A in (6). H) v_0/E_t as a function of NAD^{+} concentration (pH = 6.05) where the data was obtained from Fig. 2 in (6). In all panels, the data are represented by circles, squares, diamonds, or triangles and the model is represented by solid lines of the corresponding color.
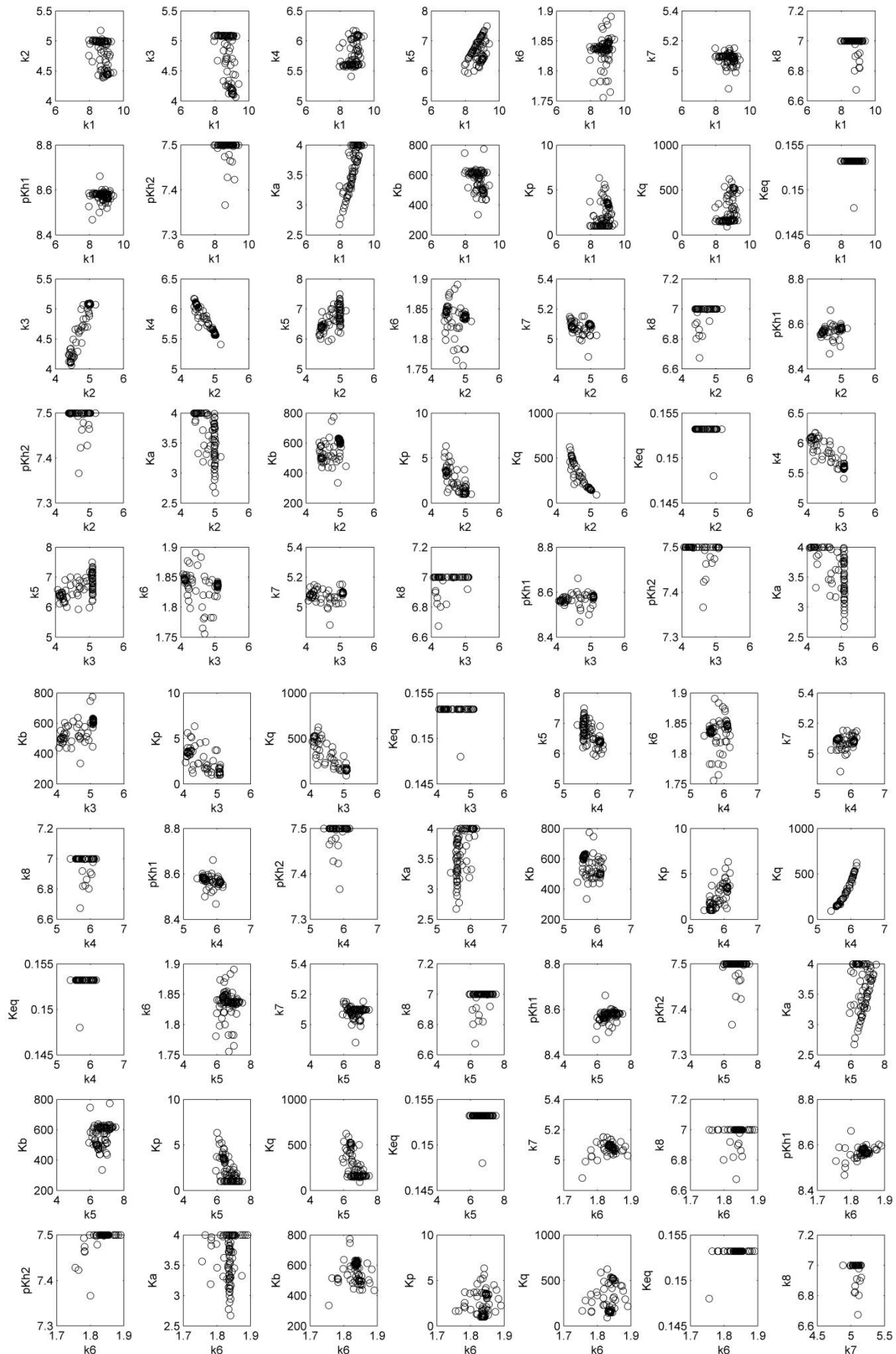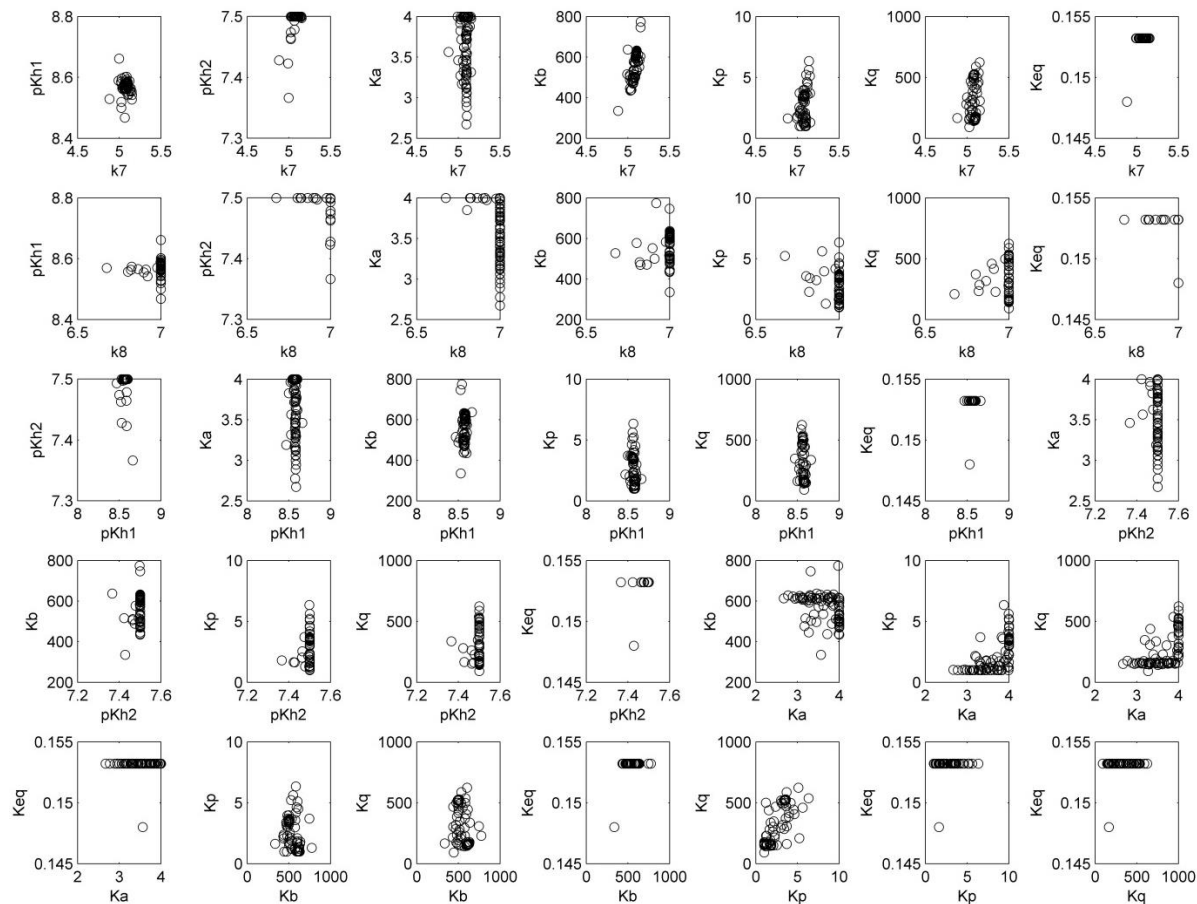
Figure S7. Scatter plots of *E. coli* E3 kinetic parameters. The kinetic parameters from 100 fits within the max/min cost value range of 1.26 shown in Figure S6 were plotted as all paired parameter combinations. K_A, K_B, K_P, and K_Q are defined as equilibrium dissociation constants for dihydrolipoamide, NAD^+, lipoamide, and NADH, respectively. The overall equilibrium constant (K_{eq}) for the reaction is defined in the main text under Model constraints. All rate constant values (k_1 through k_8) are plotted as log_{10}(rate constant), including K_A because of its large range. Rate constants and equilibrium dissociation constants are in units of min^{-1} and µM, respectively.

Table S2.

E.coli E3 observed kinetic parameter range from multiple fits to data obtained from (4-6).

[a]Parameter	Best-fit example	Min	Max	Max/Min
[b]k1 (min^{-1})	1.11×10^9	9.17×10^7	2.51×10^9	27.4
k2 (min^{-1})	2.76×10^4	2.45×10^4	1.49×10^5	6.08
k3 (min^{-1})	1.33×10^4	1.16×10^4	1.25×10^5	10.78
k4 (min^{-1})	1.25×10^6	2.57×10^5	1.49×10^6	5.78
[b]k5 (min^{-1})	2.49×10^6	8.45×10^5	3.15×10^7	37.3
k6 (min^{-1})	70.2	56.9	77.8	1.37
k7 (min^{-1})	1.21×10^5	7.62×10^4	1.42×10^5	1.87
k8 (min^{-1})	10^7	4.72×10^6	10^7	2.12
pKh1 (thiolate)	7.5	7.37	7.5	[c]1.35
pKh2 (base)	8.56	8.47	8.66	[c]1.55
K$_A$(µM)	10^4	470	10^4	21.3
K$_B$ (µM)	498	335	774	2.31
K$_P$ (µM)	3.44	1	6.34	6.34
K$_Q$ (µM)	520	92	623	6.77
Keq	0.153	0.148	0.153	1.03
[d]Fval (cost function)	0.589	0.589	0.743	1.26

[a]Rate constants were given a boundary of 10^{-3} to 10^9 min^{-1} and equilibrium dissociation constants were bounded by 1 to 10^4 µM. pKh1 and 2 were generally bounded by values between 4 and 9.
[b]These rate constants were calculated based on equilibrium detailed balance constraints derived in the methods section.
[c]The max/min values for the pKh parameter were calculated by using 10^{-pKh}.
[d]The cost function value was calculated through the weighted global sum of squares described previously (3).
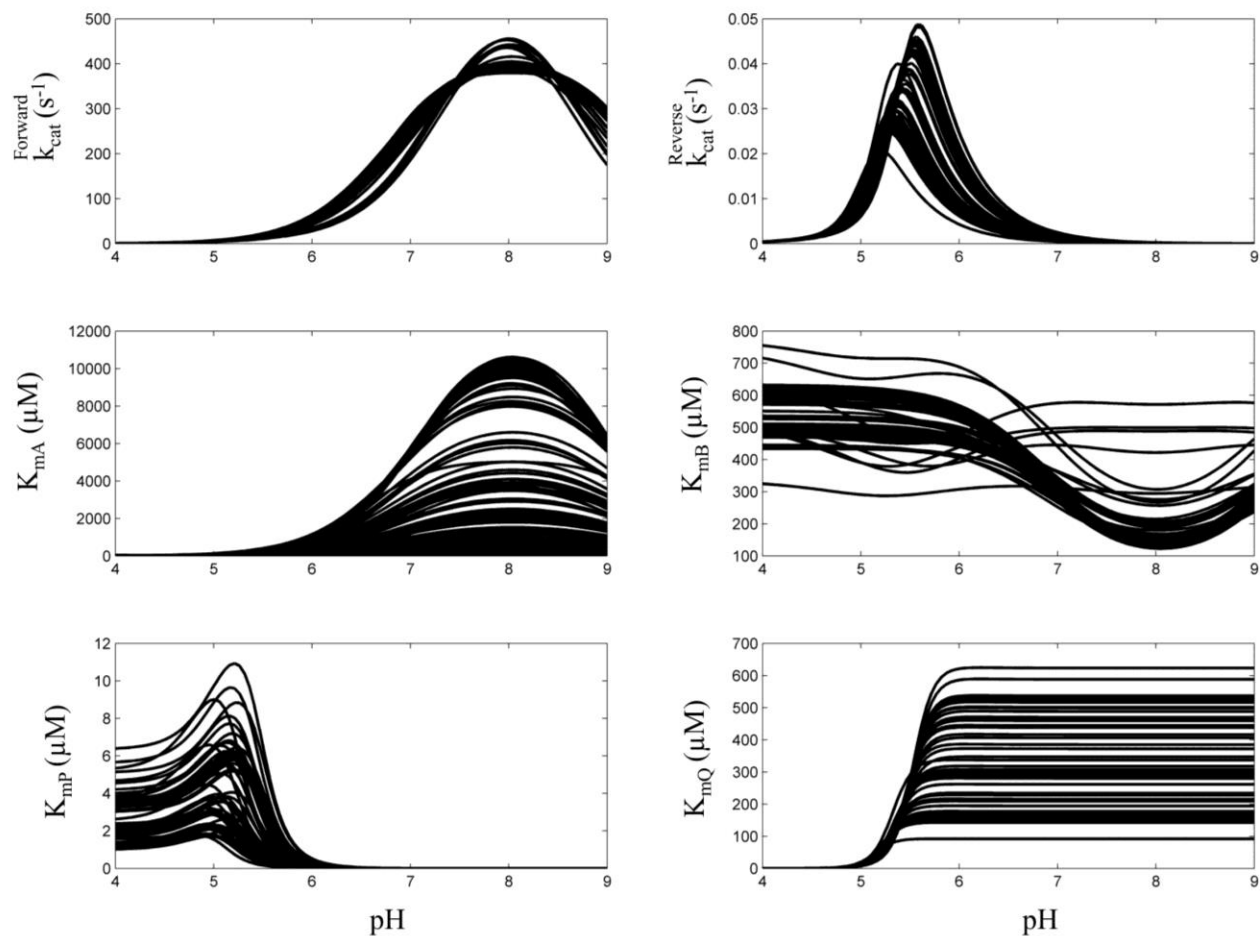
Figure S8. *E. coli* E3 calculated steady-state parameters as a function of pH using the redox independent single Kd model with all 100 parameter sets that fit the data. K_{mA}, K_{mB}, K_{mP}, and K_{mQ} are the Michaelis constants for dihydrolipoamide, NAD^+, lipoamide, and NADH, respectively.
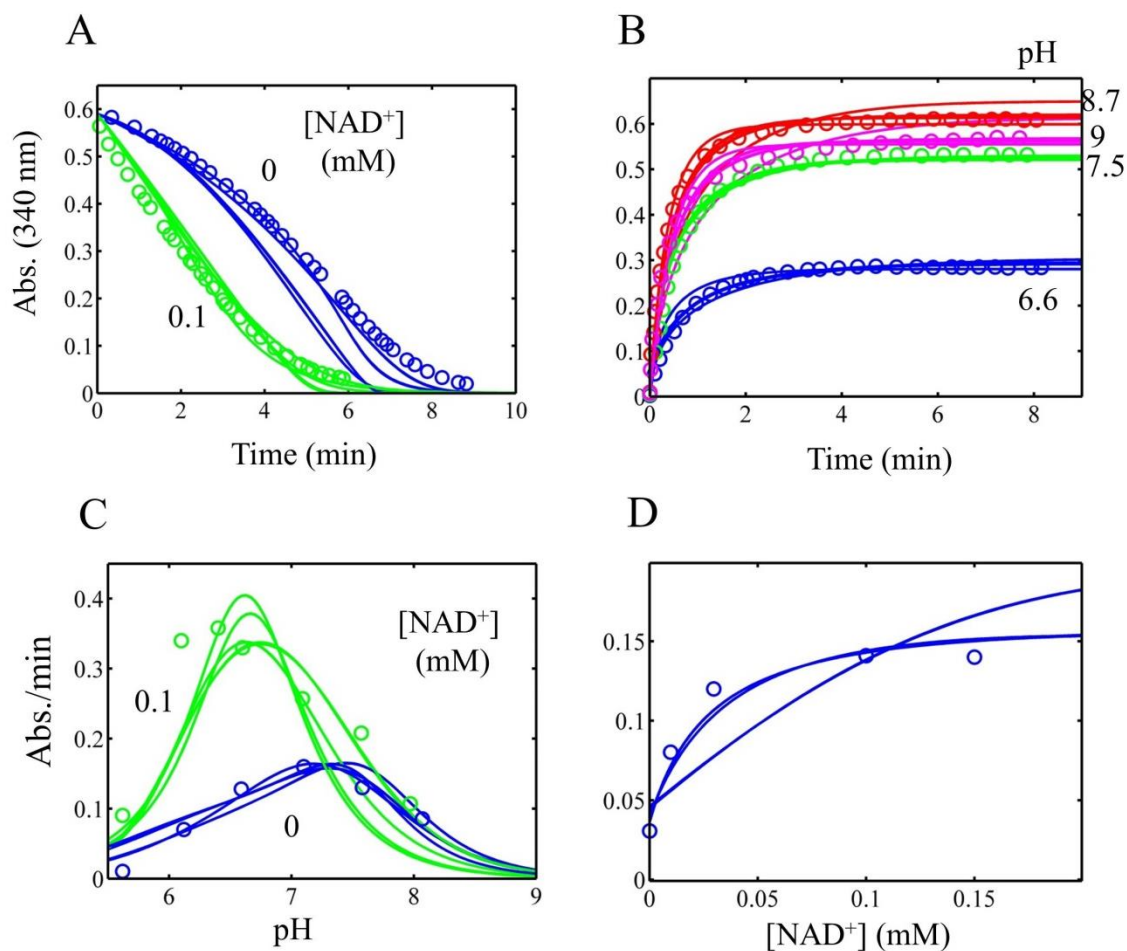
Figure S9. Multiple global fits of spinach E3 progress curves, NAD^{+} activation, and pH dependent data obtained from (7). Data were fitted to the simple redox independent K_d model through hundreds of trials of global followed by local optimization using random initial parameter values (see methods section) where 100 fits that were within fval(max)/fval(min) of 1.8 were kept. A) Progress curve data for the reverse reaction in different NAD concentrations (pH = 6.3) where the data was obtained from Fig. 4 in (7). B) Progress curve data for the forward reaction with varied pH where the data was obtained from Fig. 7 in (7). C) Initial velocity of the reverse reaction as a function of pH and NAD^{+} concentration where the data was obtained from Fig. 6 in (7). D) Activation of reverse initial velocity with increasing NAD^{+} concentration (pH = 6.3) where the data was obtained from Fig. 5 in (7). In all panels, the data are represented by circles and the model is represented by solid lines of the corresponding color.
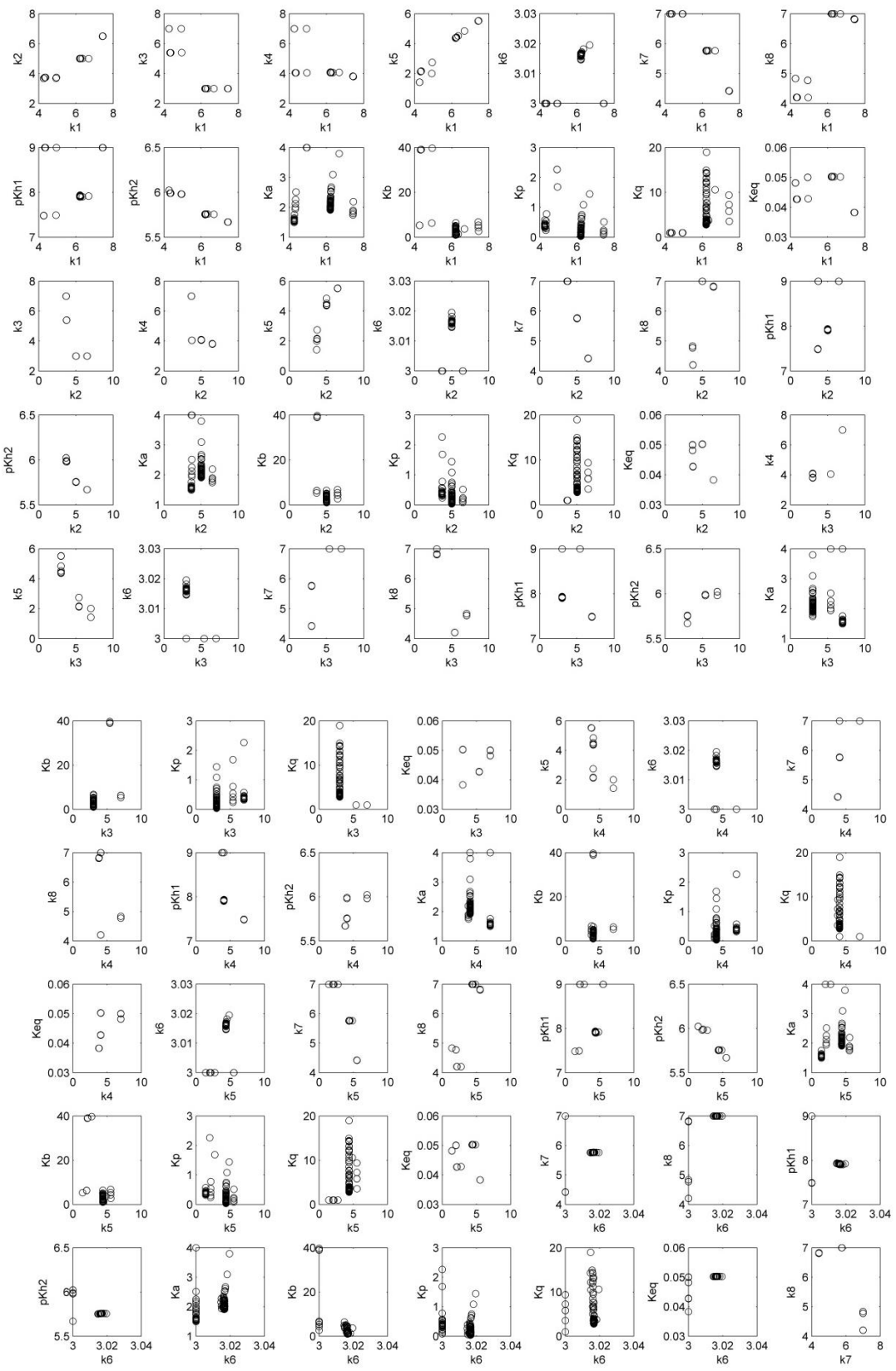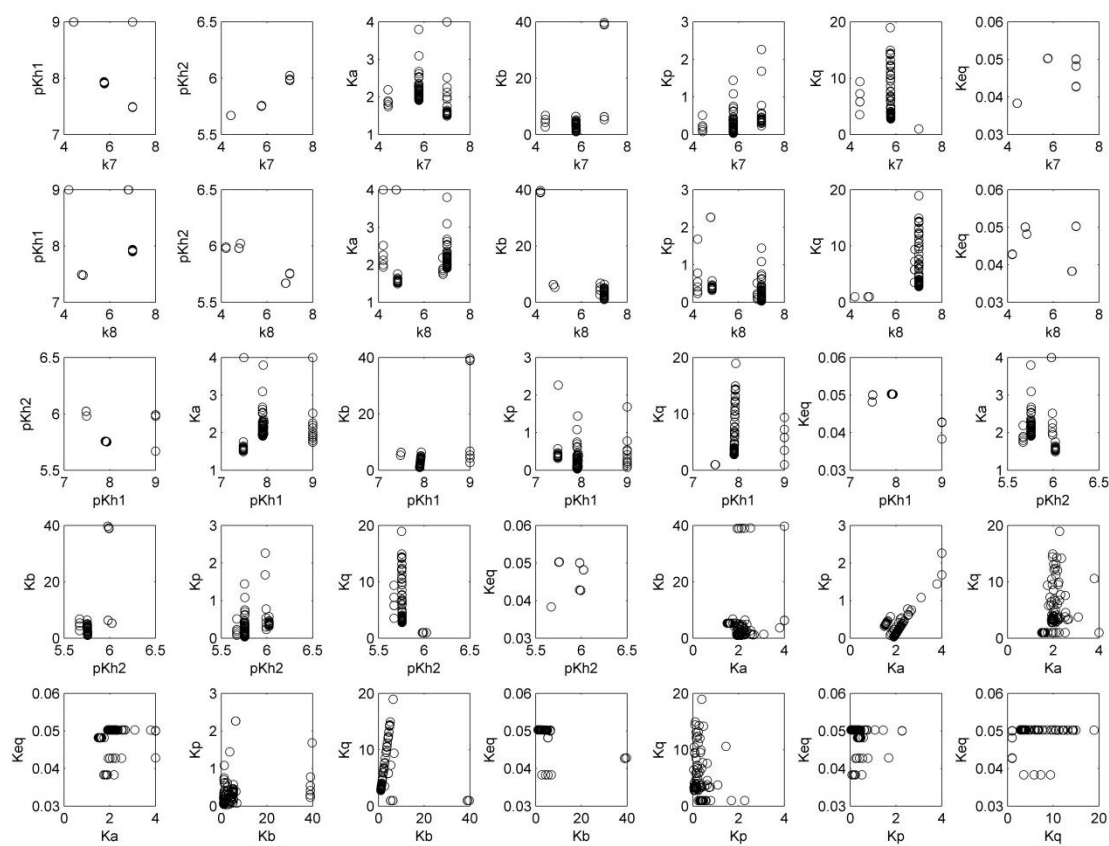
Figure S10. Scatter plots of Spinach E3 kinetic parameters. The kinetic parameters from 100 fits within the max/min cost value range of 1.79 shown in Figure S9 were plotted as all paired parameter combinations. K_A, K_B, K_P, and K_Q are defined as equilibrium dissociation constants for dihydrolipoamide, NAD^+, lipoamide, and NADH, respectively; K_{eq} is the overall equilibrium constant for the reaction defined in the main text under Model constraints. All rate constant values (k_1 through k_8), K_A, and K_P are plotted as $\log_{10}$(parameter). Rate constants and equilibrium dissociation constants are in units of min^{-1} and µM, respectively.

Table S3.

Spinach E3 observed kinetic parameter range from multiple fits to data obtained from (7).

[a]Parameter	Best-fit example	Min	Max	Max/Min
[b]k1 (min^{-1})	2.78×10^7	1.86×10^4	2.78×10^7	1.5×10^3
k2 (min^{-1})	3.17×10^6	4.80×10^3	3.17×10^6	659
k3 (min^{-1})	10^3	10^3	10^7	10^4
k4 (min^{-1})	6.33×10^3	6.33×10^3	10^7	1.58×10^3
[b]k5 (min^{-1})	3.42×10^5	26.6	3.42×10^5	1.29×10^4
k6 (min^{-1})	10^3	10^3	1.05×10^3	1.05
k7 (min^{-1})	2.60×10^4	2.60×10^4	10^7	384
k8 (min^{-1})	6.43×10^6	1.6×10^4	10^7	626
pKh1 (thiolate)	5.67	5.67	6.02	[c]2.26
pKh2 (base)	9	7.48	9	[c]33.1
K_A (µM)	155	31.3	10^4	320
K_B (µM)	2.70	1	39.7	39.7
K_P (µM)	3.26	1.08	185	170
K_Q (µM)	3.55	1	18.9	18.9
Keq	0.05	0.0383	0.0503	1.31
[d]Fval (cost function)	0.713	0.713	1.28	1.79

[a]Rate constants were given a boundary of 10^{-3} to 10^9 min^{-1} and equilibrium dissociation constants were bounded by 1 to 10^4 µM. pKh1 and 2 were generally bounded by values between 4 and 9.
[b]These rate constants were calculated based on equilibrium detailed balance constraints derived in the methods section.
[c]The max/min values for the pKh parameter were calculated by using 10^{-pKh}.
[d]The cost function value was calculated through the weighted global sum of squares described previously (3).
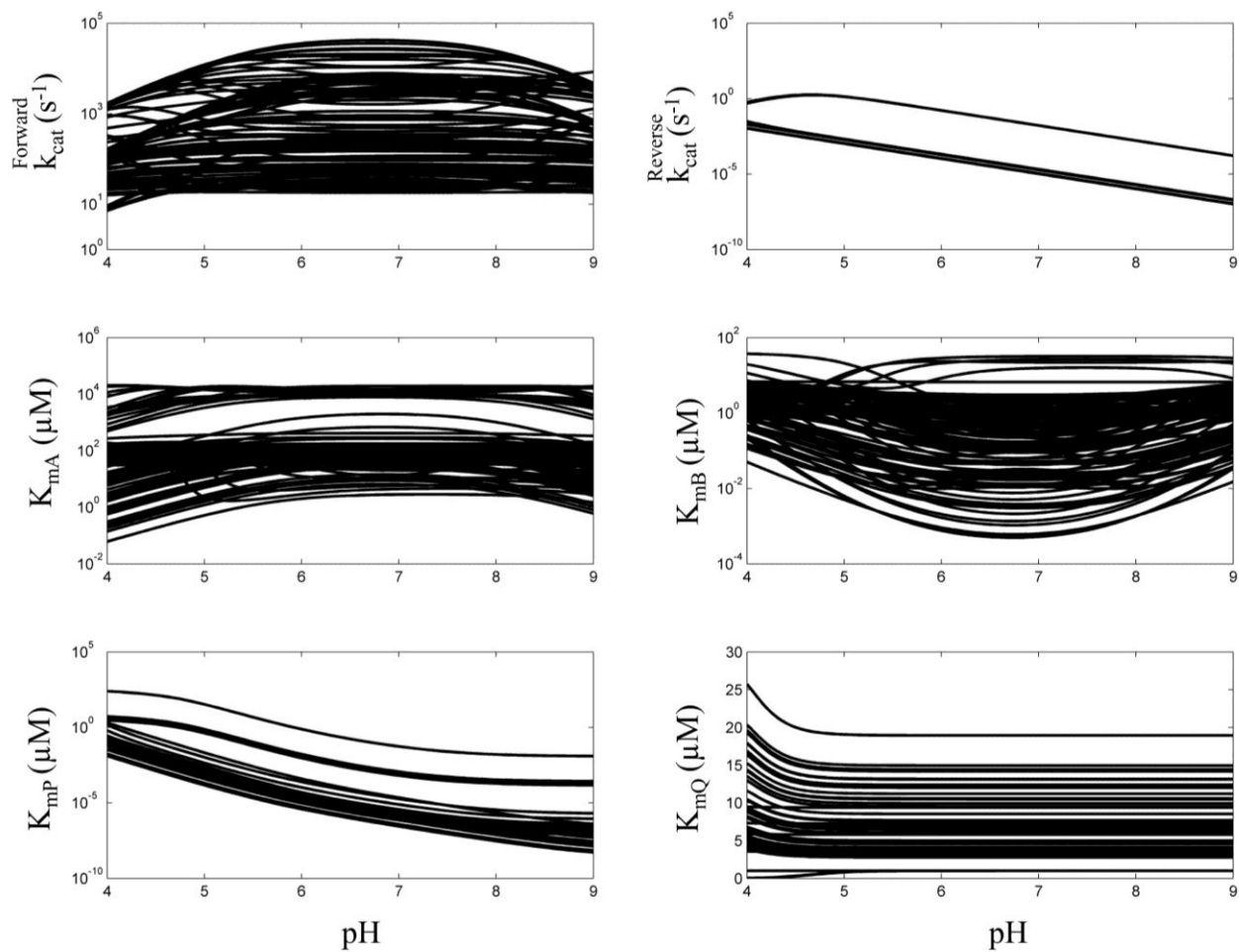
Figure S11. Spinach E3 calculated steady-state parameters as a function of pH using the redox independent single Kd model with all 100 parameter sets that fit the data. K_{mA}, K_{mB}, $K_{mP,}$ and K_{mQ} are the Michaelis constants for dihydrolipoamide, NAD^+, lipoamide, and NADH, respectively.
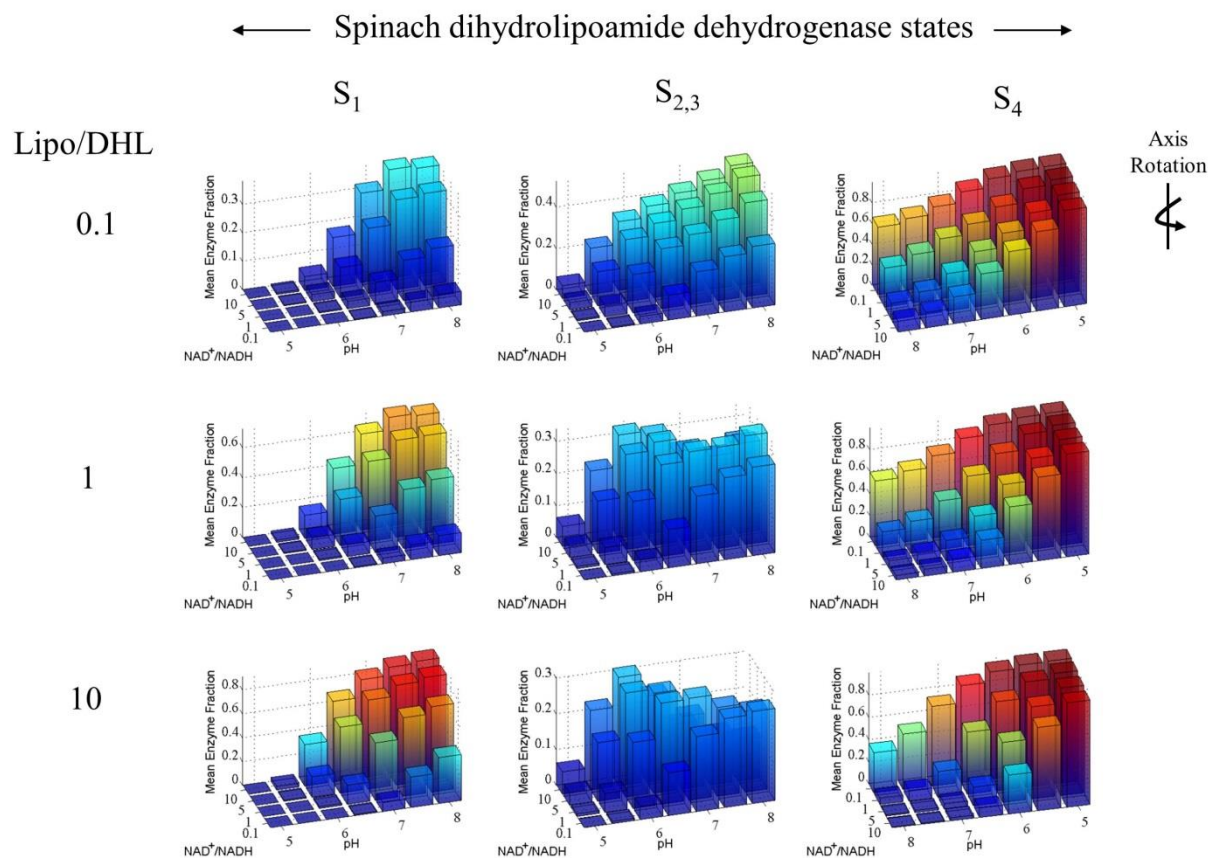
`

Figure S12. Mean spinach E3 major steady-state distributions. Spinach E3 major steady-state distributions calculated from 100 parameter sets with the redox independent K_d model and lipoamide/dihydrolipoamide (Lipo/DHL) and NAD^+/NADH ratios as a function of pH. Total concentrations of lipoamide and NAD species were set equal to 10 mM and 3 mM respectively. The total lipoamide concentration is based on a millimolar range approximation of the stoichiometry and volume of the pyruvate dehydrogenase complex (8). The total concentration of NAD species was chosen to compare with human liver state distribution calculations shown in Fig. 7. Note that plots in the S_3 column have been rotated with respect to other columns to better view smaller bars that would be hidden otherwise.
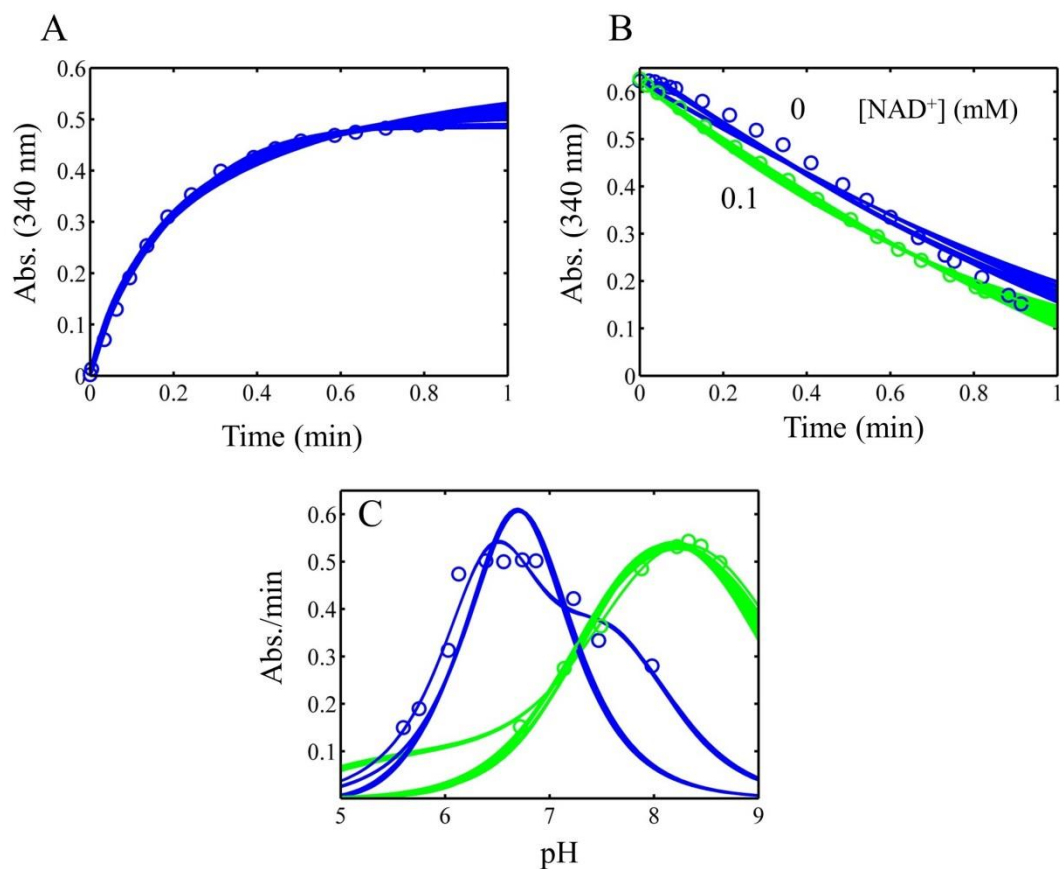
Figure S13. Multiple global fits of human liver E3 progress curve and pH dependent data where the data was obtained from (9). Data were fitted to the simple redox independent K_d model through hundreds of trials of global followed by local optimization using random initial parameter values (see methods section) where 70 fits that were within fval(max)/fval(min) of 3.94 were kept. A) Progress curve data for the forward reaction (pH = 8.5) where the data was obtained from Fig. 6 of (9). B) Progress curve data for the reverse reaction in different NAD^+ concentrations (pH = 6.5) where the data was obtained from Fig. 4 of (9). C) Initial velocity as a function of pH for the forward (green) and reverse reaction (blue) where the data was obtained from Fig. 5 of (9). In all panels, the data are represented by circles and the model is represented by solid lines of the corresponding color.
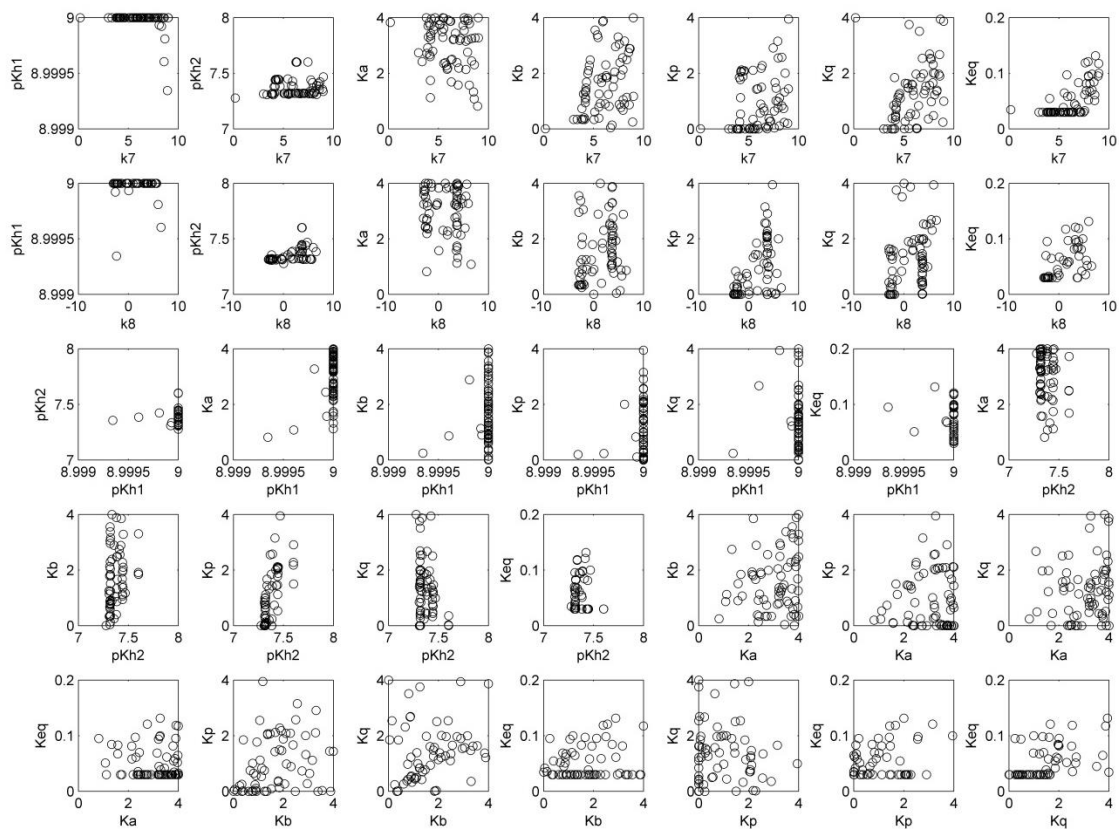
Figure S14. Scatter plots of Human E3 kinetic parameters. The kinetic parameters from 70 fits within the max/min cost value range of 3.94 shown in Figure S13 were plotted as all paired parameter combinations. K_A, K_B, K_P, and K_Q are defined as equilibrium dissociation constants for dihydrolipoamide, NAD^+, lipoamide, and NADH, respectively. The overall equilibrium constant (K_{eq}) for the reaction is defined in the main text under Model constraints. All rate constant values (k_1 through k_8) and equilibrium dissociation constants are plotted as $\log_{10}$(parameter). Rate constants and equilibrium dissociation constants are in units of min^{-1} and μM, respectively.

Table S4.

Human liver E3 observed kinetic parameter range from multiple fits to data obtained from (9).

[a]Parameter	Best-fit example	Min	Max	Max/Min
[b]k1 (min^{-1})	4.83×10^5	2.15×10^4	1.29×10^8	6×10^3
k2 (min^{-1})	1.01×10^5	10^3	3.06×10^6	3.06×10^3
k3 (min^{-1})	9.87×10^3	8.02×10^3	10^9	1.25×10^5
k4 (min^{-1})	2.08×10^4	1.32×10^4	10^9	7.6×10^4
[b]k5 (min^{-1})	2.18×10^{-7}	6.4×10^{-13}	10^8	1.68×10^{20}
k6 (min^{-1})	10^{-3}	10^{-3}	10^9	10^{12}
k7 (min^{-1})	1.18×10^8	0.159	10^9	6.3×10^9
k8 (min^{-1})	1.14×10^4	10^{-3}	10^9	10^{12}
pKh1 (thiolate)	7.32	5.6	7.6	[c]101
pKh2 (base)	9	7.55	9	[c]28.5
K_A (µM)	581	1.12	10^4	9×10^3
K_B (µM)	4.0	1	10^4	10^4
K_P (µM)	34	1	9×10^3	9×10^3
K_Q (µM)	3.2	1	9.12×10^3	9.12×10^3
Keq	0.106	0.0300	0.118	3.92
[d]Fval (cost function)	0.266	0.266	1.05	3.94

[a]Rate constants were given a boundary of 10^{-3} to 10^9 min^{-1} and equilibrium dissociation constants were bounded by 1 to 10^4 µM. pKh1 and 2 were generally bounded by values between 4 and 9.
[b]These rate constants were calculated based on equilibrium detailed balance constraints derived in the methods section.
[c]The max/min values for the pKh parameter were calculated by using 10^{-pKh}.
[d]The cost function value was calculated through the weighted global sum of squares described previously (3).
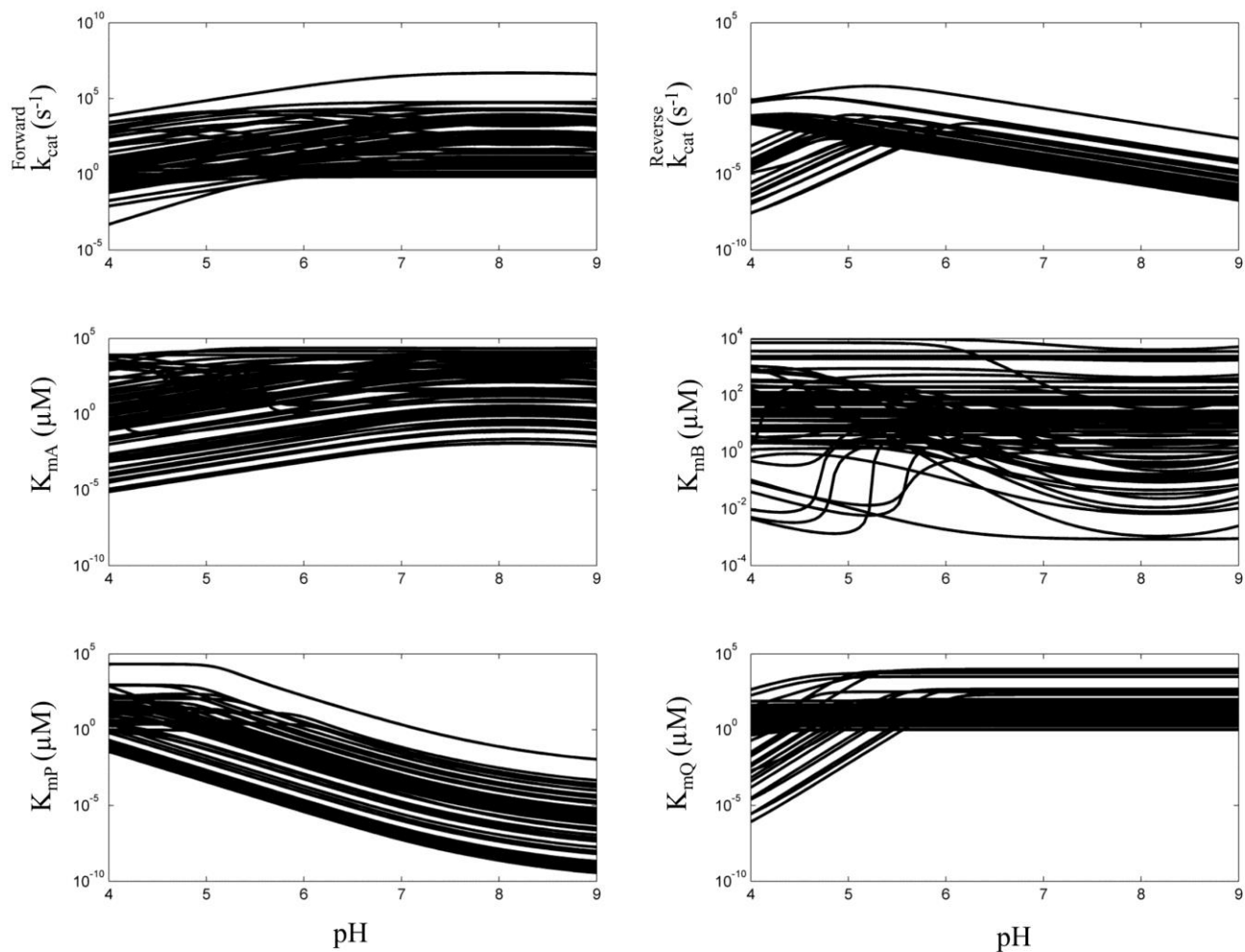
Figure S15. Human liver E3 calculated steady-state parameters as a function of pH using the redox independent single Kd model with all 70 parameter sets that fit the data. K_{mA}, K_{mB}, K_{mP}, and K_{mQ} are the Michaelis constants for dihydrolipoamide, NAD^+, lipoamide, and NADH, respectively.
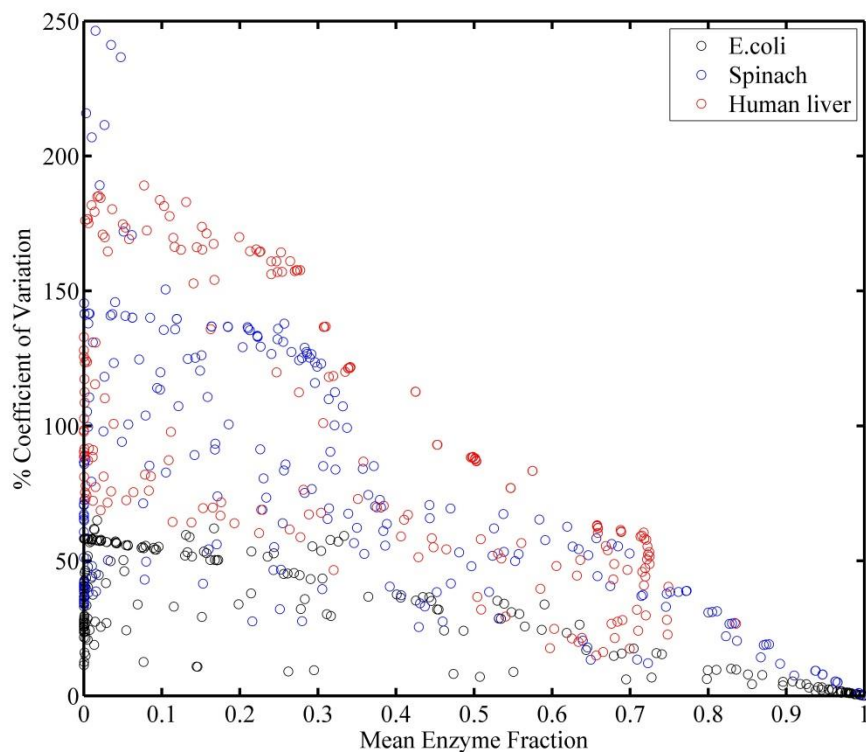
Figure S16. Variation of E3 enzyme redox steady-state distribution in the conditions shown in Figs. 6 and 7 of the main text for *E.coli* and human liver respectively, and in Fig. S12 for spinach E3. The mean and standard deviation of the steady-state redox state distributions were calculated to compute the percent coefficient of variation (%CV) as follows %CV = 100*(std. dev /mean). The %CV for the distributions follows the general trend of human > spinach > *E.coli*. This calculation also shows that the most populated enzyme states, or states with the greatest mean enzyme fraction, have the smallest %CV.

Supporting References

1. Reed, J. K. 1973. Studies on the kinetic mechanism of lipoamide dehydrogenase from rat liver mitochondria. The Journal of biological chemistry 248:4834-4839.

2. Massey, V. 1960. The identity of diaphorase and lipoyl dehydrogenase. Biochimica et biophysica acta 37:314-322.

3. Bazil, J. N., K. C. Vinnakota, F. Wu, and D. A. Beard. 2013. Analysis of the kinetics and bistability of ubiquinol:cytochrome c oxidoreductase. Biophysical journal 105:343-355.

4. Wilkinson, K. D. and C. H. Williams, Jr. 1981. NADH inhibition and NAD activation of Escherichia coli lipoamide dehydrogenase catalyzing the NADH-lipoamide reaction. The Journal of biological chemistry 256:2307-2314.

5. Koike, M., P. C. Shah, and L. J. Reed. 1960. alpha-Keto acid dehydrogenation complexes. III. Purification and properties of dihydrolipoic dehydrogenase of Escherichia coli. The Journal of biological chemistry 235:1939-1943.

6. Sahlman, L. and C. H. Williams, Jr. 1989. Lipoamide dehydrogenase from Escherichia coli. Steady-state kinetics of the physiological reaction. The Journal of biological chemistry 264:8039-8045.

7. Matthews, J. and L. J. Reed. 1963. Purification and properties of a dihydrolipoic dehydrogenase from Spinacia oleracea. The Journal of biological chemistry 238:1869-1876.

8. Perham, R. N. 2000. Swinging arms and swinging domains in multifunctional enzymes: catalytic machines for multistep reactions. Annu Rev Biochem 69:961-1004.

9. Ide, S., T. Hayakawa, K. Okabe, and M. Koike. 1967. Lipoamide dehydrogenase from human liver. The Journal of biological chemistry 242:54-60.